

SUPPORTING INFORMATION

Dimethyl amino phenyl substituted Silver Phthalocyanine as UV- and Visible-Light Absorbing Photoinitiator: *In-situ* Preparation of Silver/Polymer Nanocomposites

Louise Breloy,^a Yusuf Alcay,^b Ismail Yilmaz*,^b Martin Breza,^c Julie Bourgon,^a Vlasta Brezova,^c Yusuf Yagci*,^b Davy-Louis Versace*^a

^a Institut de Chimie et des Matériaux Paris-Est (ICMPE) – UMR-CNRS7182-UPEC, 2-8, rue Henri Dunant, 94320 Thiais, France

^b Istanbul Technical University, Department of Chemistry, Maslak, Istanbul, 34469, Turkey

^c Slovak University of Technology in Bratislava, Institute of Physical Chemistry and Chemical Physics, Department of Physical Chemistry, Radlinského 9, SK-812 37 Bratislava, Slovak Republic

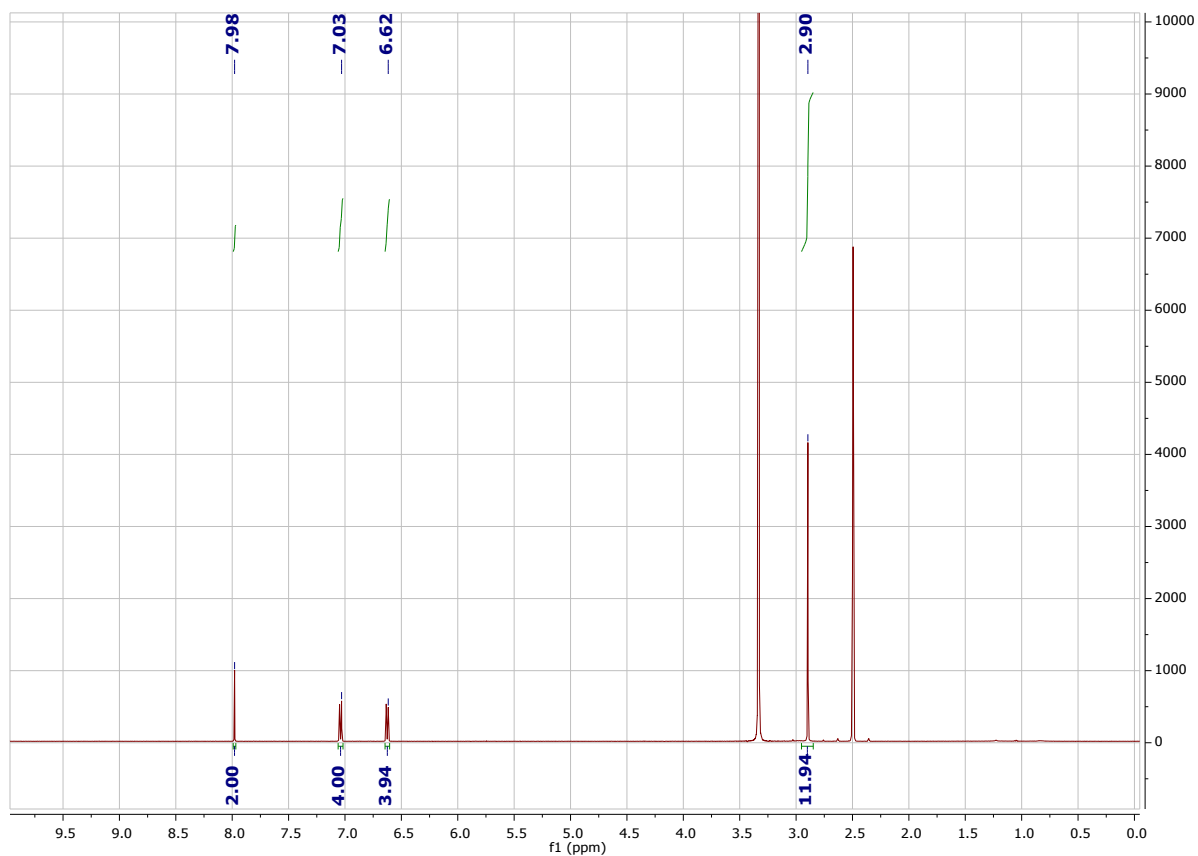


Figure S1. ¹H-NMR spectrum of 1

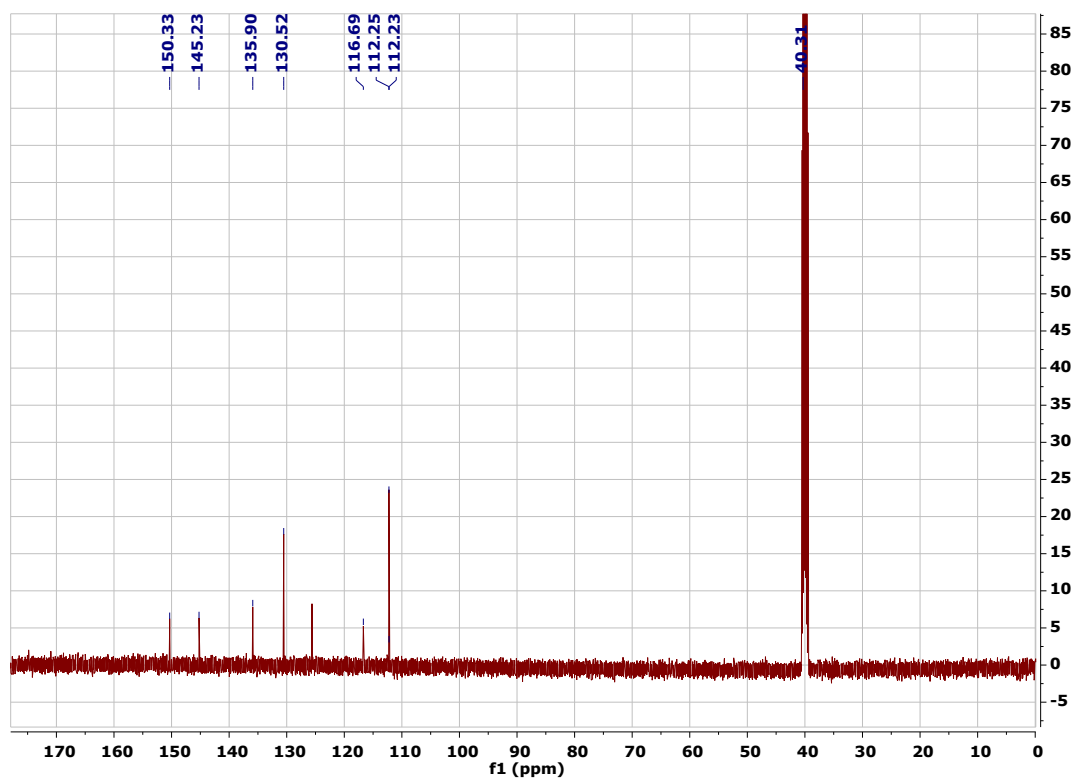


Figure S2. ^{13}C -NMR spectrum of **1**

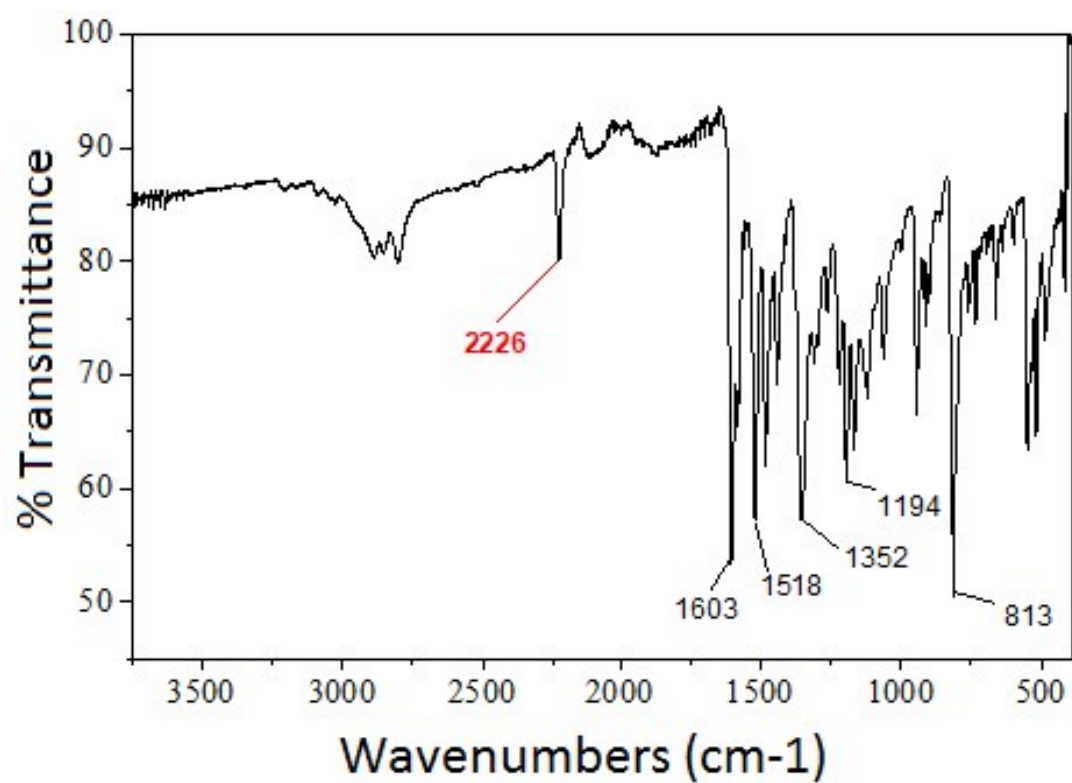


Figure S3. FT-IR spectrum of **1**.

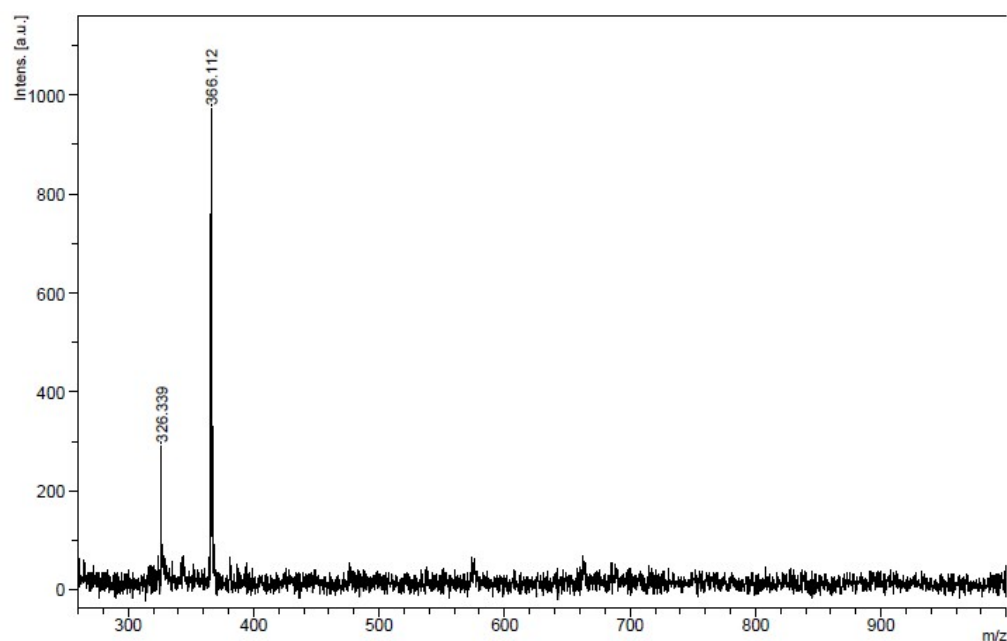


Figure S4. MALDI-TOF spectrum of **1**

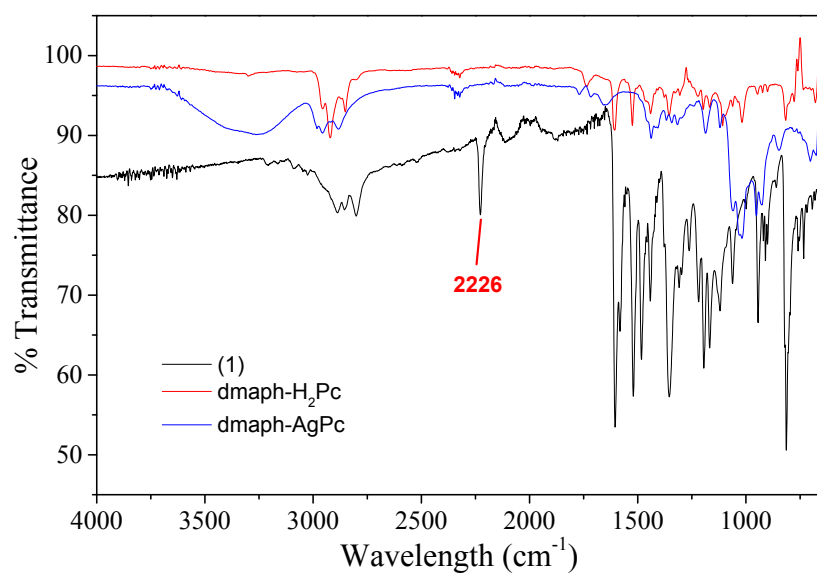


Figure S5. FT-IR spectra of (1), dmaph-Ag^(II)Pc and dmaph-H₂Pc.

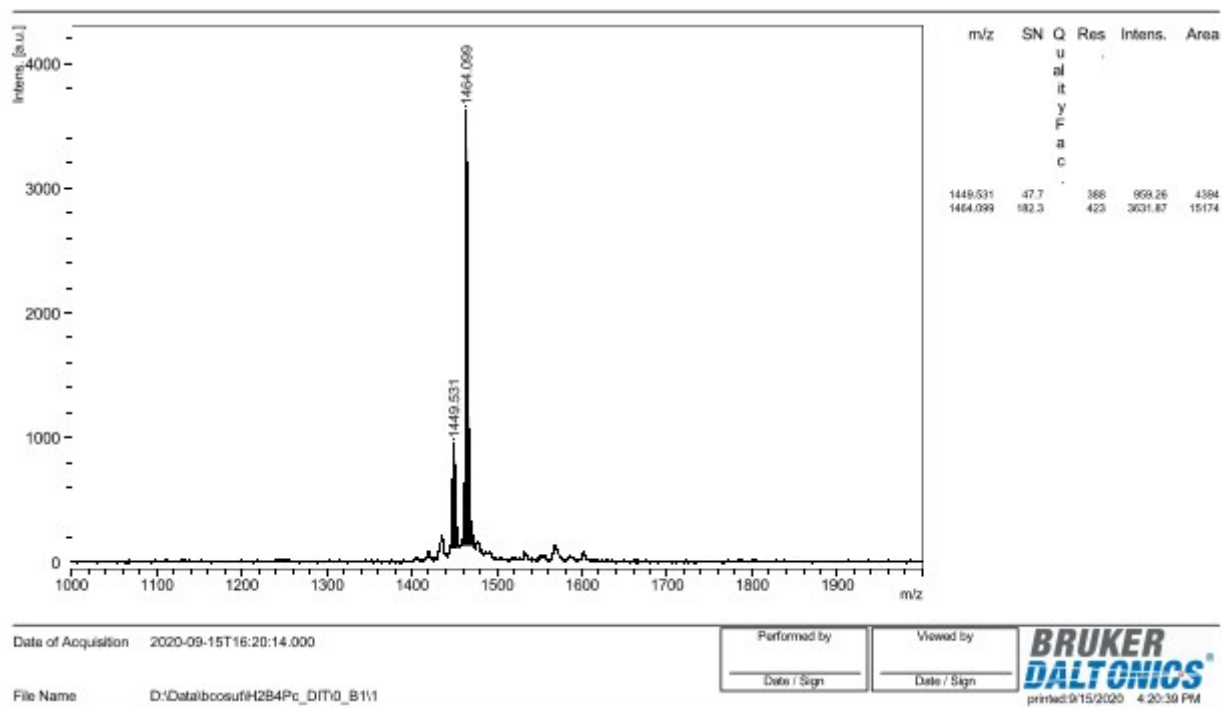


Figure S6. MALDI-TOF spectrum of dmaph-H₂Pc

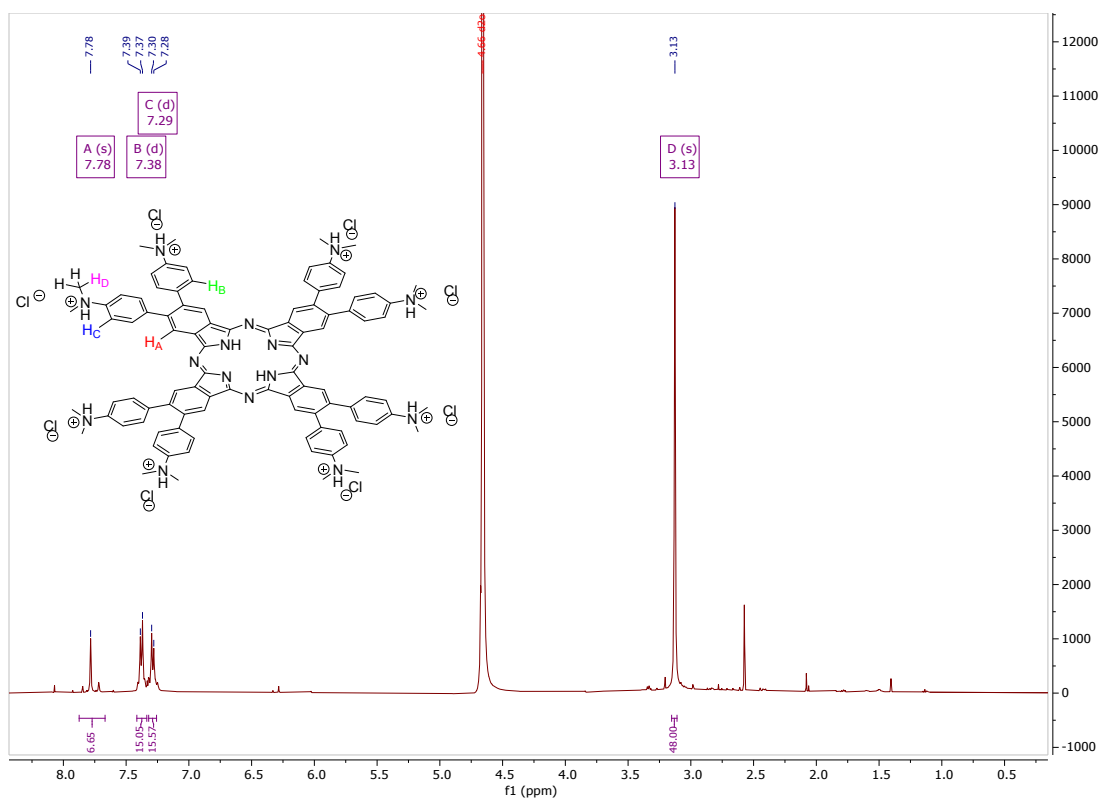
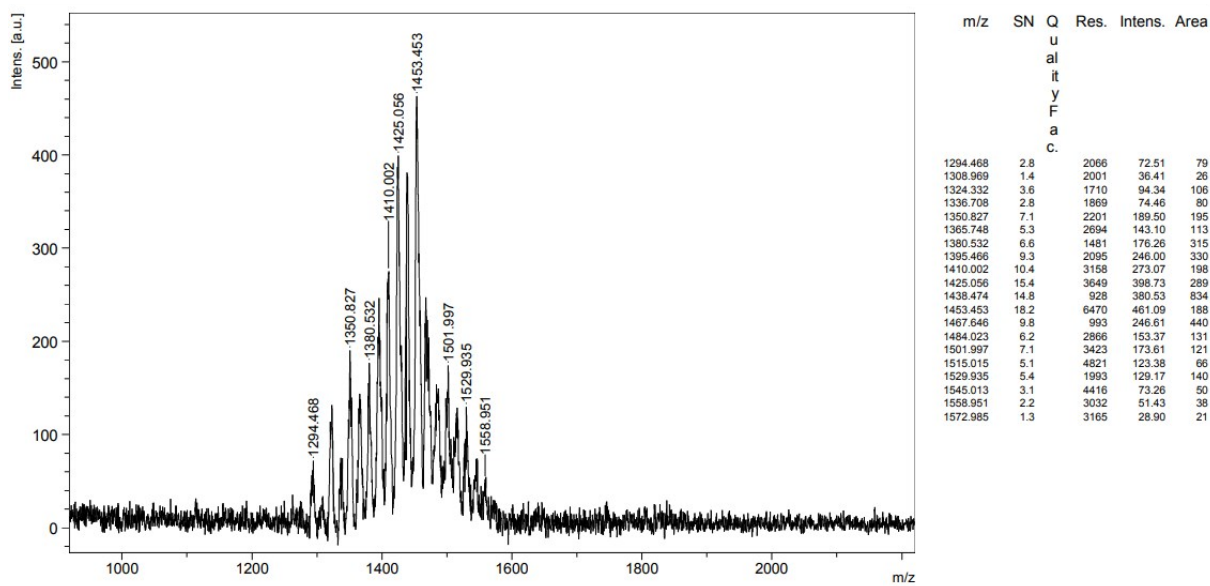


Figure S7. $^1\text{H-NMR}$ spectrum of $\text{dmaph-H}_2\text{Pc-nHCl}$



Date of Acquisition 2019-11-07T13:33:55.000

File Name D:\Data\lbcosut\5_NOM\0_D8\1

Performed by

Viewed by

Date / Sign

Date / Sign

BRUKER DALTONICS[®]

printed:11/7/2019 1:34:40 PM

Figure S8. MALDI-TOF spectrum of $\text{dmaph-Ag}^{(II)}\text{Pc}$.

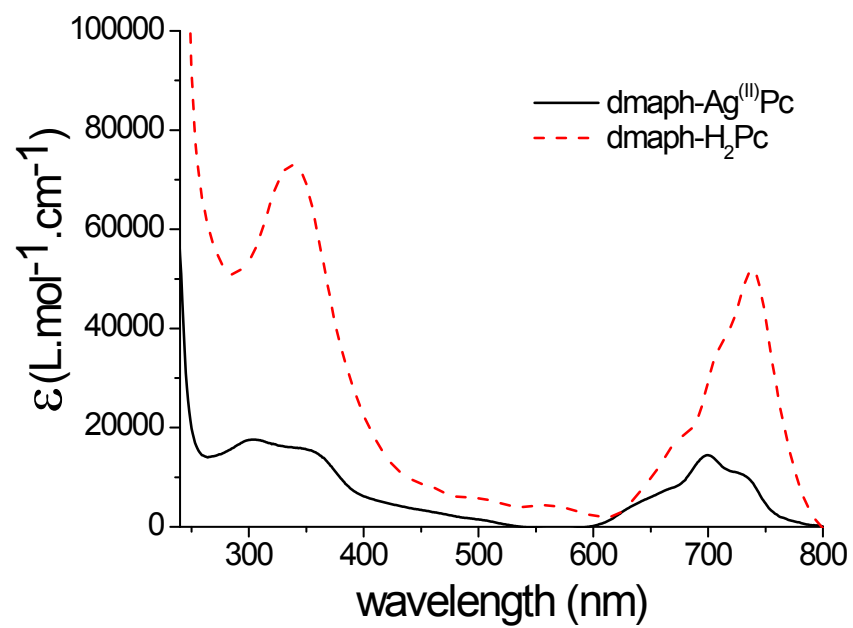


Figure S9. UV-Vis spectra of **dmaph-Ag^(I)Pc** and **dmaph-H₂Pc** in CHCl₃.

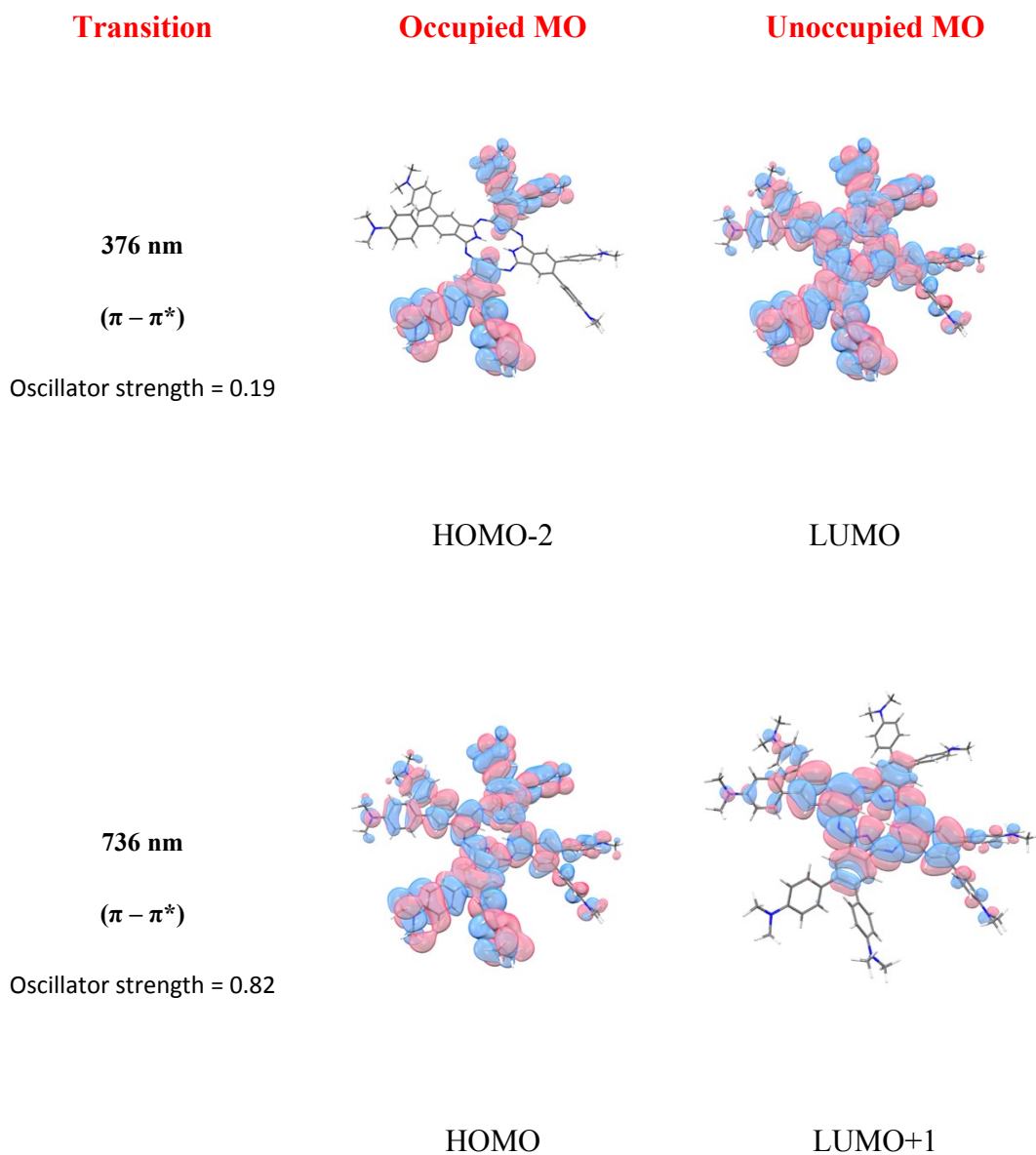


Figure S10. Selected MOs of **dmaph-H₂Pc** obtained by B3LYP method.

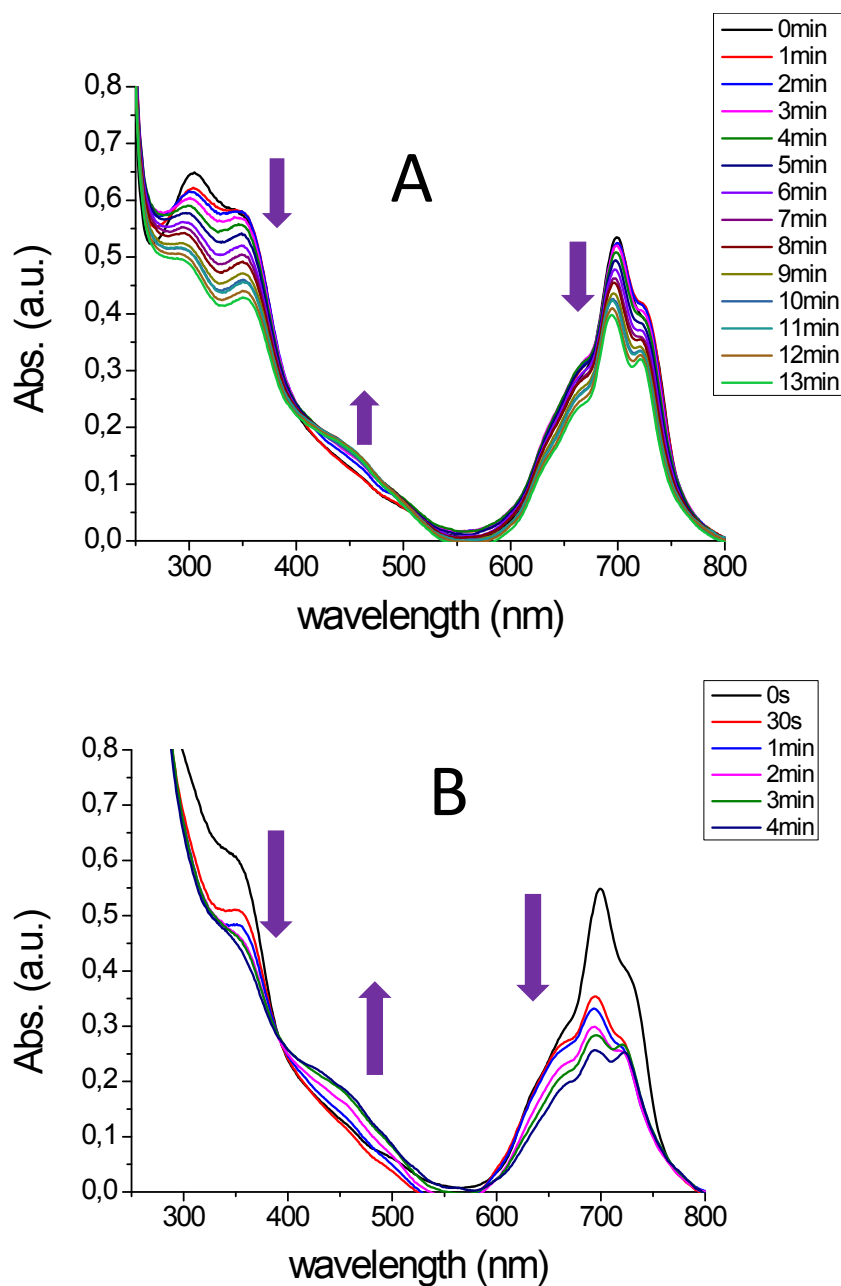


Figure S11. Photolysis of A) **dmaph-Ag^(I)Pc** and B) **dmaph-Ag^(I)Pc/Iod** under LED@405nm irradiation. LED@405 nm intensity = 390 mW/cm². [Iod] = 7.9×10^{-5} M, [**dmaph-Ag^(I)Pc**] = 3.8×10^{-5} M. Solvent = CHCl₃.

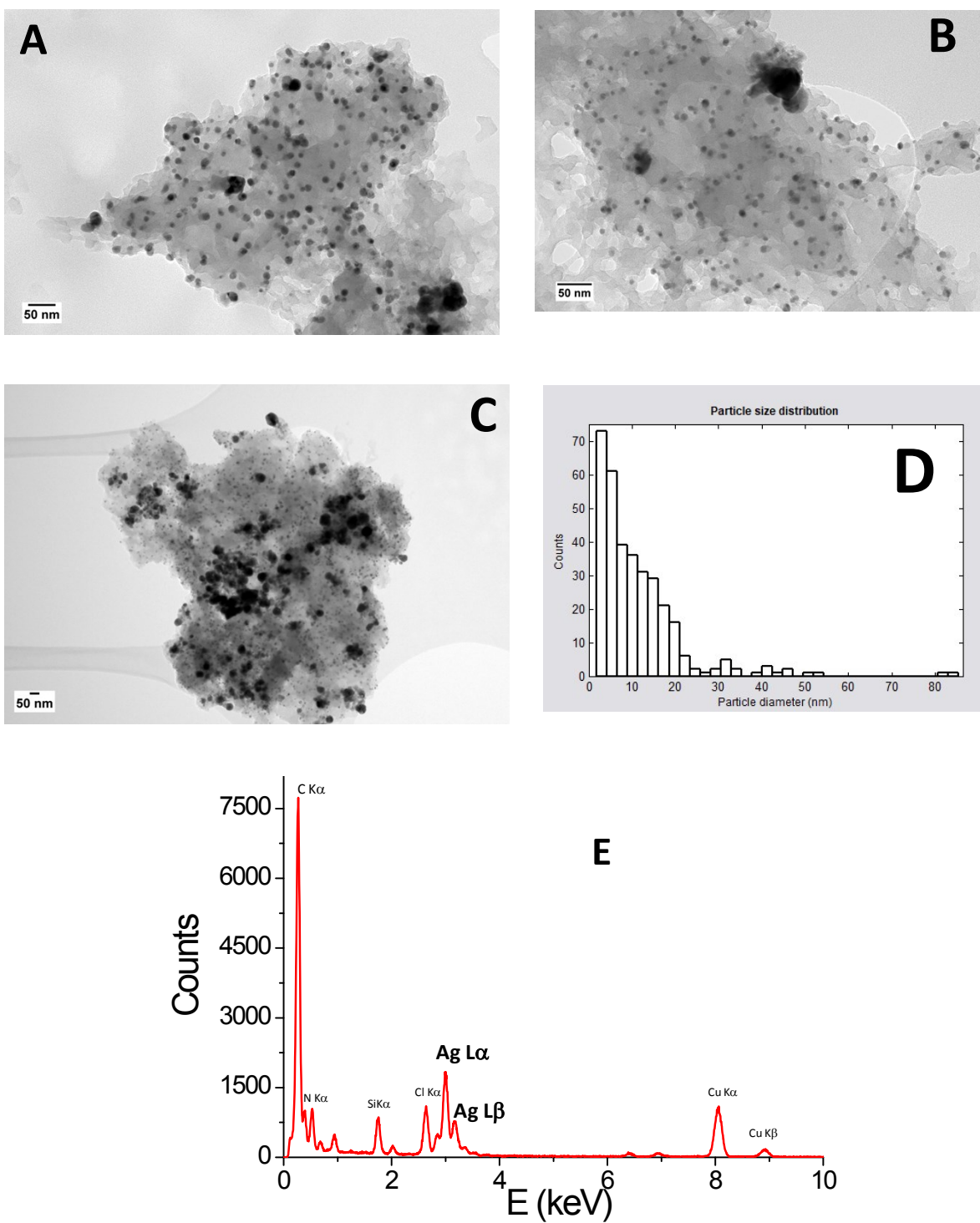


Figure S12. A), B) and C) TEM images of Ag NPs after irradiation (LED@385 nm) of **dmaph-Ag^(II)Pc/Iod** photoinitiating system in CHCl₃. D) Particulate size diameter (in nm) and E) EDX spectrum of Ag NPs. [**dmaph-Ag^(II)Pc**] = 3.9×10^{-5} M and [Iod] = 8.4×10^{-5} M.

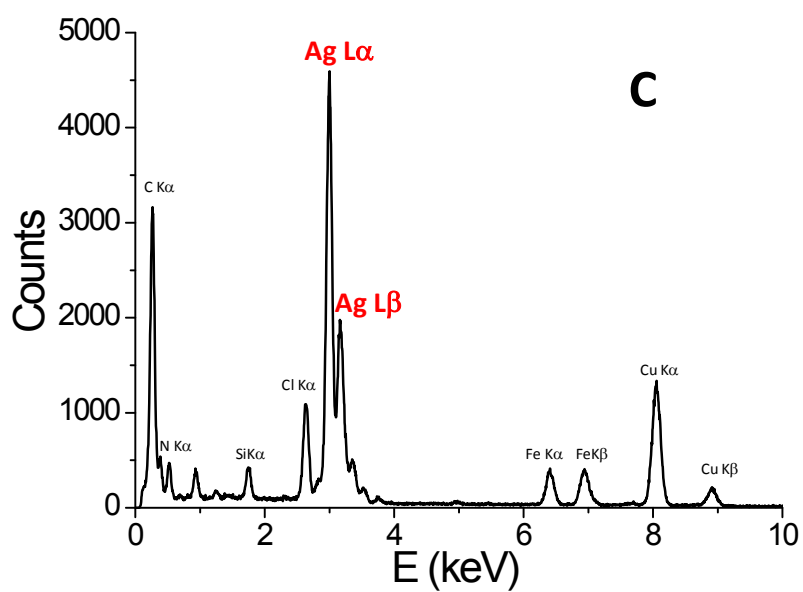
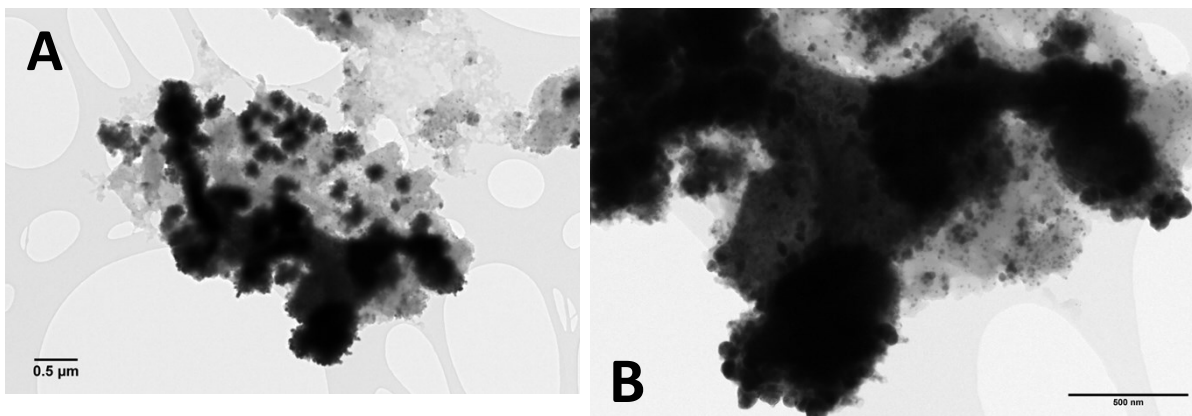


Figure S13. A) and B) TEM images of Ag NPs after irradiation (LED@385 nm) of **dmaph-Ag^(II)Pc** in CHCl₃. C) EDX spectrum of Ag NPs. [**dmaph-Ag^(II)Pc**] = 3.9×10^{-5} M.

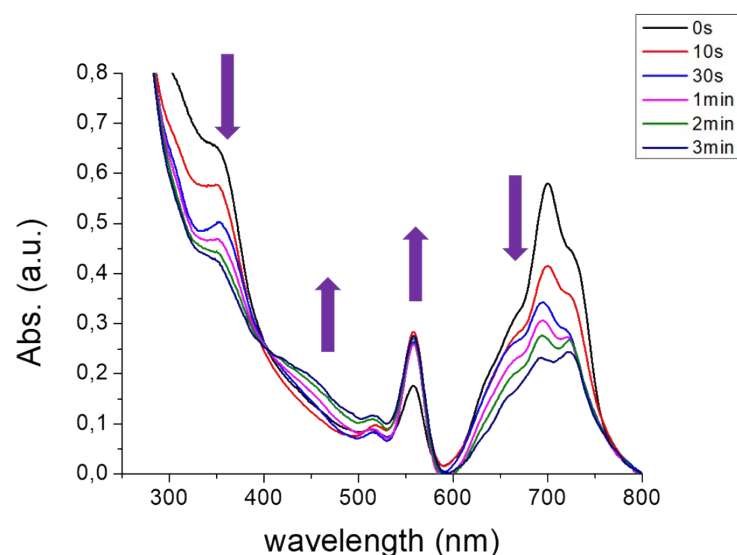


Figure S14. Photolysis of **dmaph-Ag^(I)Pc/Iod/RhB** under LED@385nm irradiation. LED@385 nm intensity = 470 mW/cm². [**dmaph-Ag^(I)Pc**] = 1.4×10^{-5} M. [Iod] = 7.9×10^{-5} M. [RhB] = 2.3×10^{-6} M. Solvent = CHCl₃.

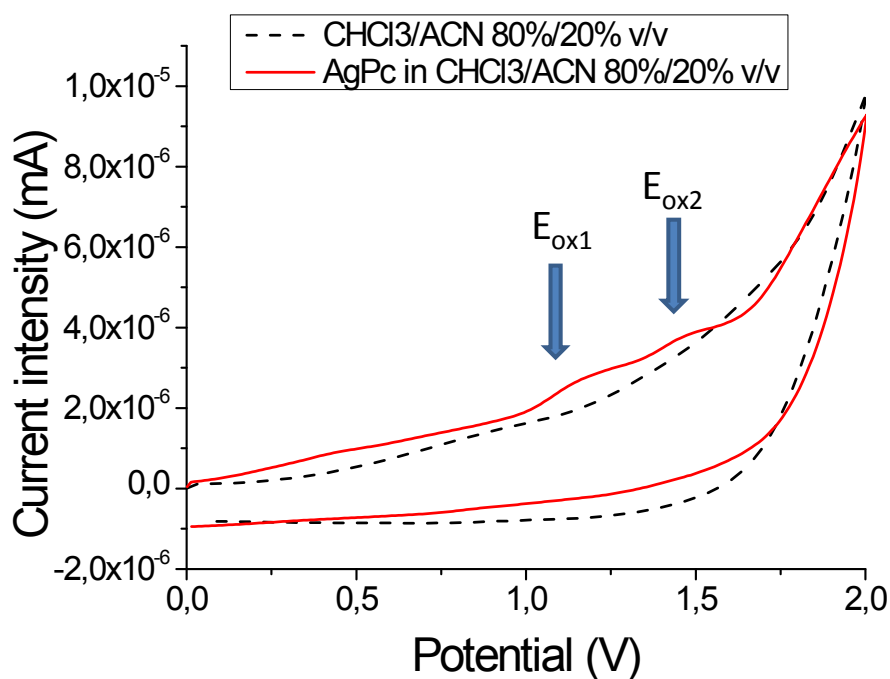


Figure S15. Cyclic voltammograms of **dmaph-Ag^(I)Pc** in a mixed solvent CHCl₃/ACN (80/20 v/v) + 5×10^{-2} M *n*Et₄BF₄ measured at a scan rate of 25 mV.s⁻¹. [**dmaph-Ag^(I)Pc**] = 10^{-4} M.

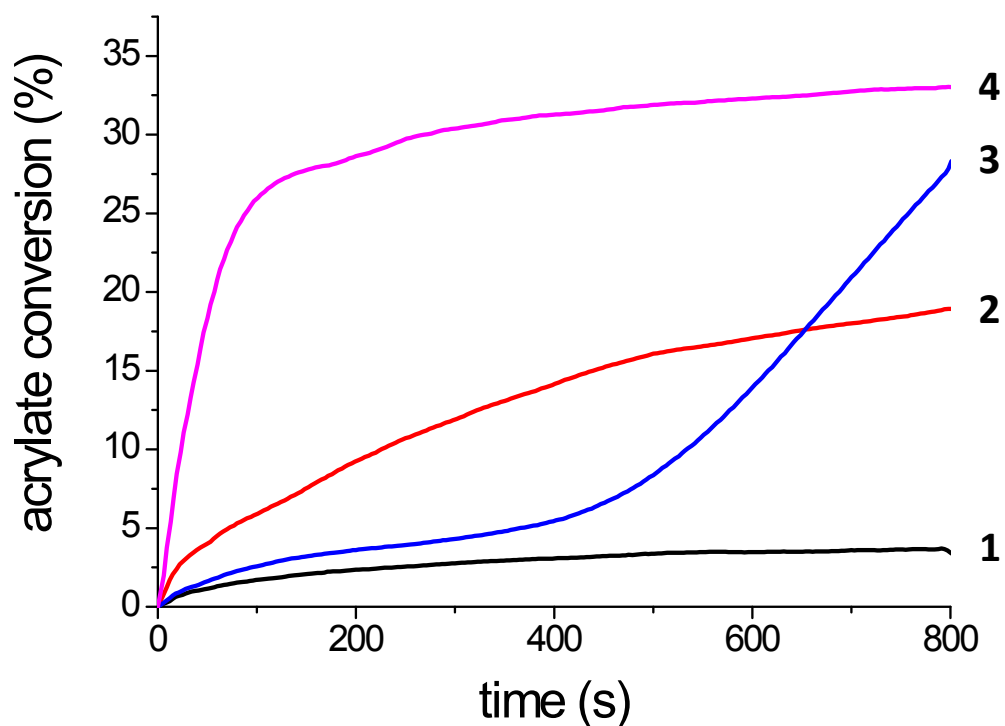


Figure S16. Kinetic profiles of TMPTA in laminate with **dmaph-Ag^(II)Pc** (0.25 wt%) and **dmaph-Ag^(II)Pc/Iod** (0.25%/2.5% w/w) under LED exposure. 1) **dmaph-Ag^(II)Pc/TMPTA** upon LED@385 nm, 2) **dmaph-Ag^(II)Pc/TMPTA** upon LED@405 nm, 3) **dmaph-Ag^(II)Pc/Iod/TMPTA** upon LED@385 nm and 4) **dmaph-Ag^(II)Pc/Iod/TMPTA** upon LED@405 nm.

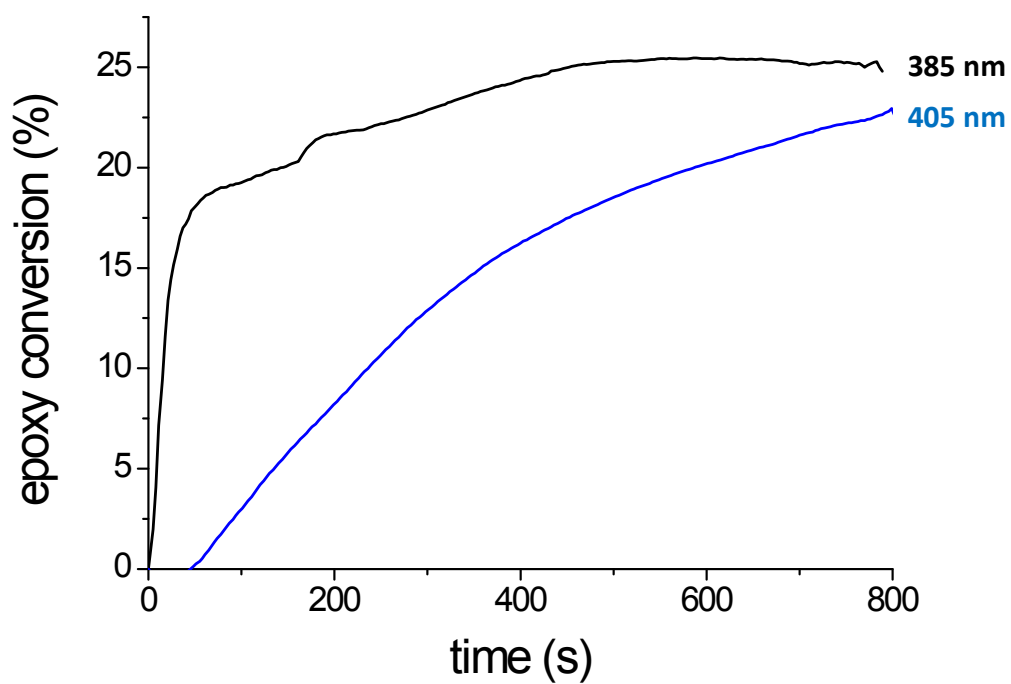


Figure S17. Kinetics of ring-opening polymerization of EPOX/CHO (50%/50% w/w) under air with **dmaph-Ag^(II)Pc** (0.25%wt) upon LEDs irradiation at 385 nm (130 mW/cm²) and at 405 nm (160 mW/cm²).

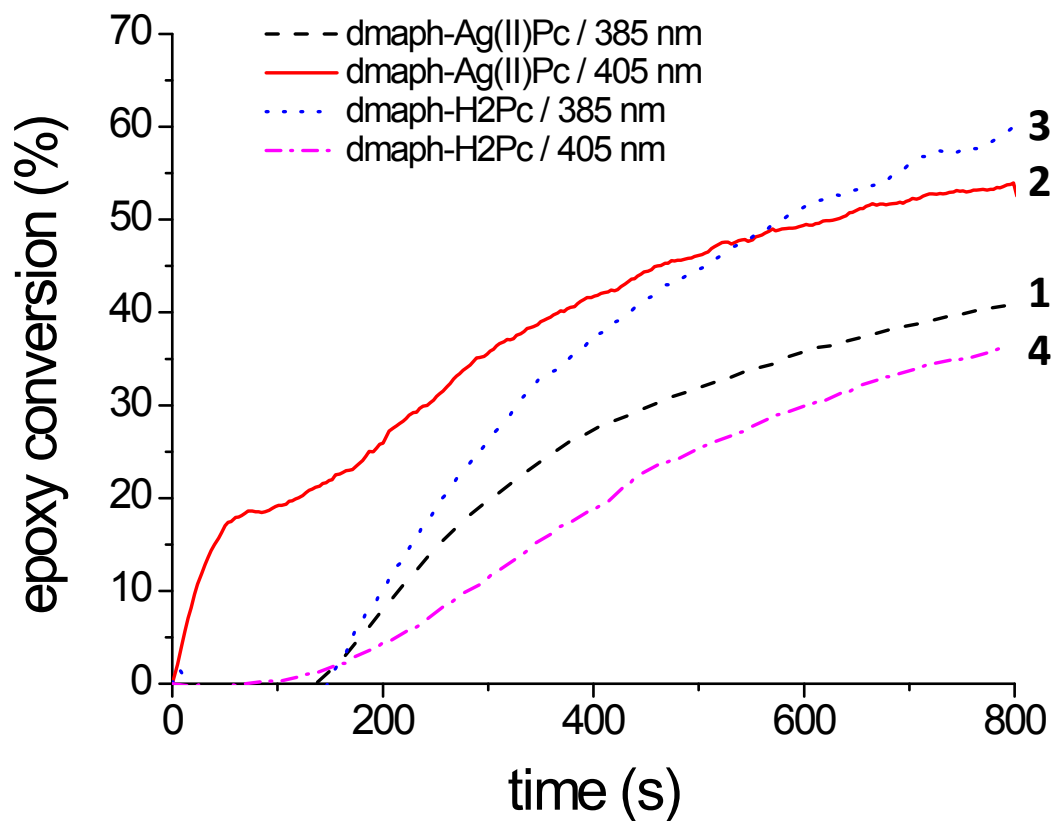


Figure S18. Kinetics of photopolymerization of EPOX/CHO (50/50 wt%) under air with **dmaph-Ag^(II)Pc**/Iod (0.25%/2.5% w/w) under 1) LED@385 nm, 2) LED@405 nm exposure and with **dmaph-H2Pc**/Iod (0.25%/2.5% w/w) under 3) LED@385 nm and 4) LED@405 nm. Intensities of LED@385 nm and LED@405 nm are respectively 130 and 160 mW/cm².

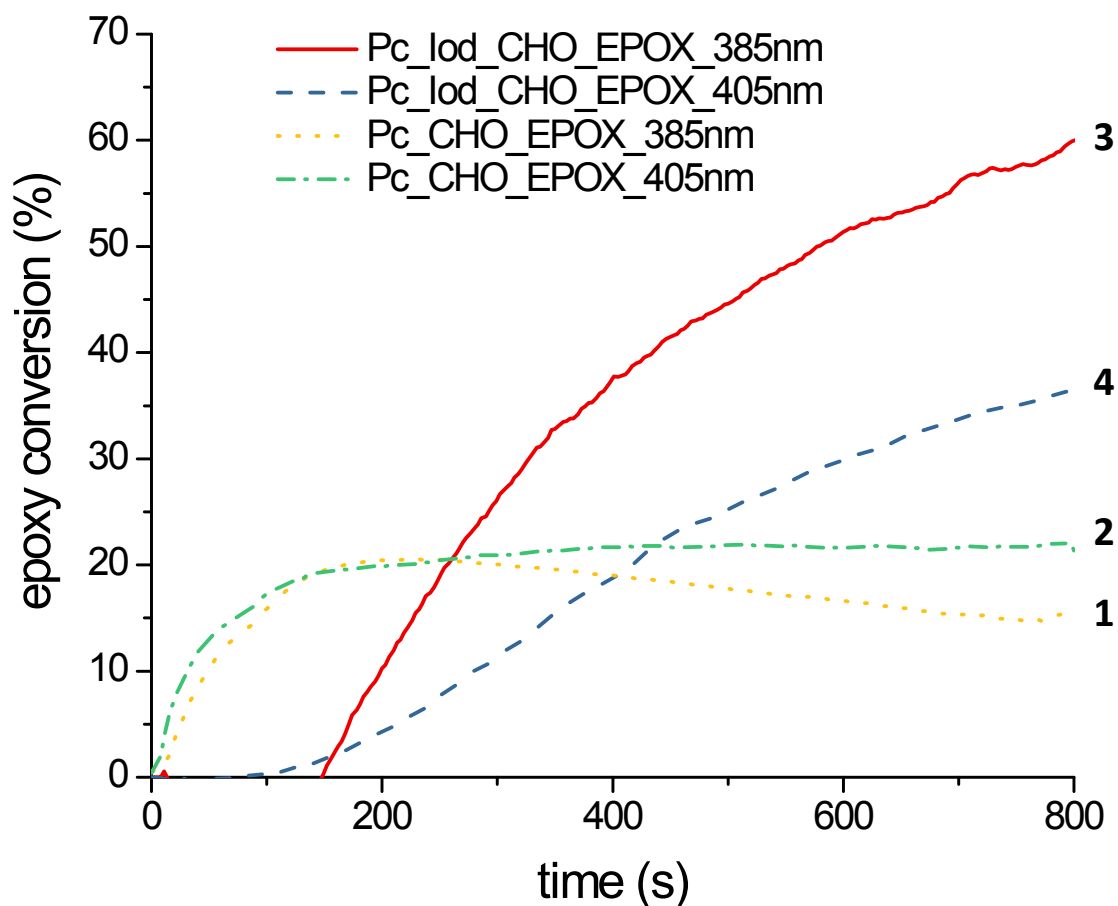


Figure S19. Kinetics of photopolymerization of EPOX/CHO (50/50 wt%) under air with **dmaph-H2Pc** alone (0.25 wt%) under 1) LED@385 nm, 2) LED@405 nm exposure and with **dmaph-H2Pc/Iod** (0.25%/2.5% w/w) under 3) LED@385 nm and 4) LED@405 nm. Intensities of LED@385 nm and LED@405 nm are respectively 130 and 160 mW/cm².

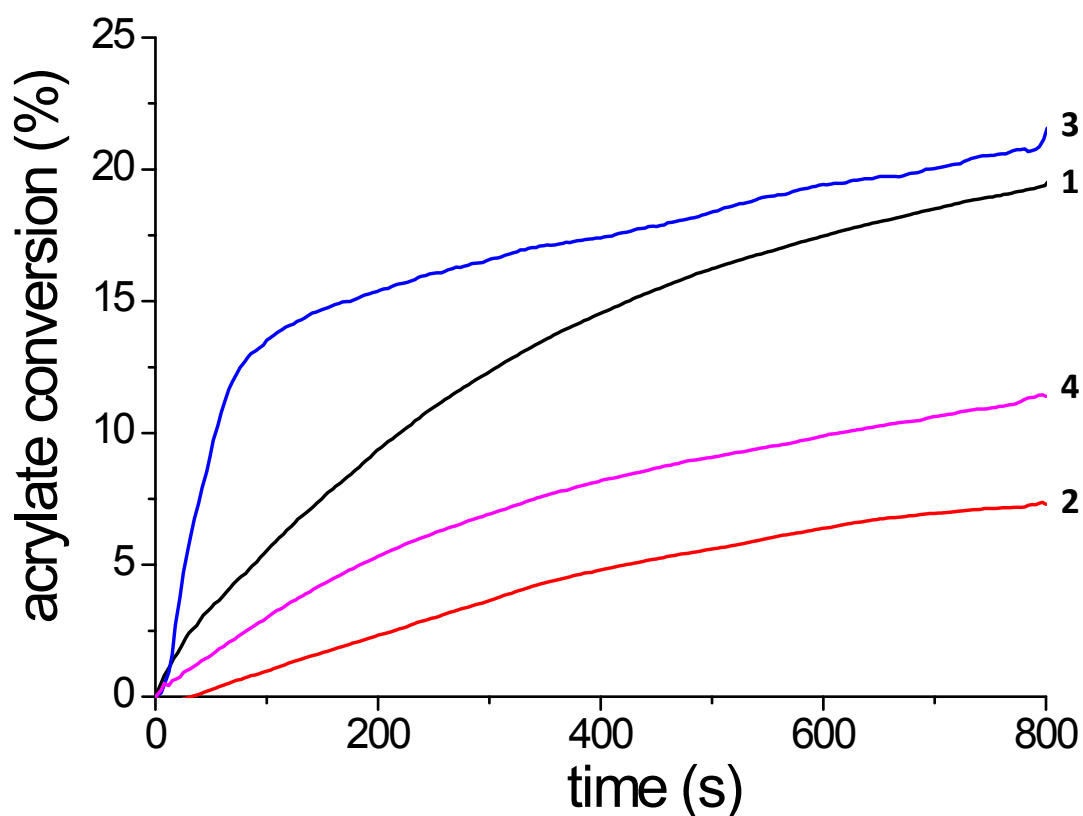


Figure S20. Kinetic profiles of TMPTA in laminate with **dmaph-H2Pc** (0.25 wt%) and **dmaph-H2Pc/Iod** (0.25%/2.5% w/w) under LED exposure. 1) **dmaph-H2Pc**/TMPTA upon LED@385 nm, 2) **dmaph-H2Pc**/TMPTA upon LED@405 nm, 3) **dmaph-H2Pc/Iod**/TMPTA upon LED@385 nm and 4) **dmaph-H2Pc/Iod**/TMPTA upon LED@405 nm. Intensities of LED@385 nm and LED@405 nm are respectively 130 and 160 mW/cm².

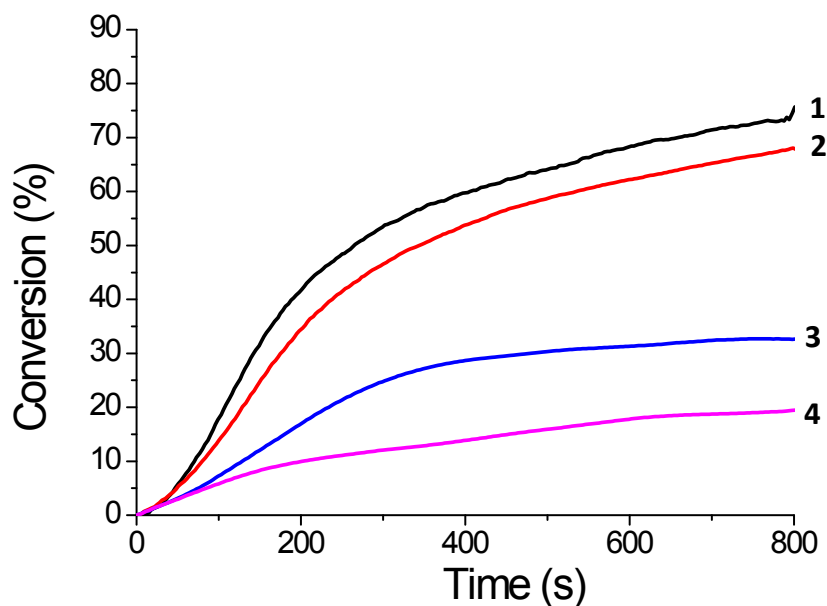


Figure S21. Kinetic profiles of the system **dmaph-Ag^(I)Pc/Iod/EPOX/CHO/TMPTA** (0.25%/2.5%/33%/33%/33% w/w/w/w/w) in laminate. Epoxy and acrylate conversions of EPOX/CHO (curves 1 and 2) and TMPTA (curves 3 and 4) respectively with **dmaph-Ag^(I)Pc/Iod** (0.25%/2.5% w/w) photoinitiating system upon LEDs irradiation at 385 nm (130 mW/cm², curves 1 and 3) and at 405 nm (160 mW/cm², curves 2 and 4).

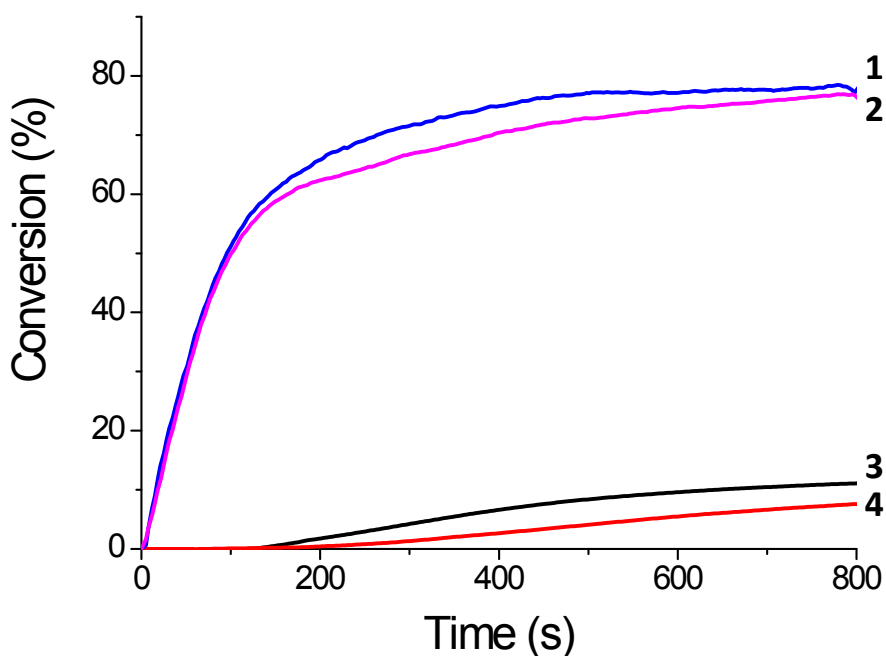


Figure S22. Kinetic profiles of the system **dmaph-Ag^(I)Pc/Iod/EPOX/CHO/TMPTA** (0.25%/2.5%/33%/33%/33% w/w/w/w/w) under air. Epoxy and acrylate conversions of EPOX/CHO (curves 1 and 2) and TMPTA (curves 3 and 4) respectively with **dmaph-**

$\text{Ag}^{\text{II}}\text{Pc}$ /Iod (0.25%/2.5% w/w) photoinitiating system upon LEDs irradiation at 385 nm (130 mW/cm², curves 1 and 3) and at 405 nm (160 mW/cm², curves 2 and 4).

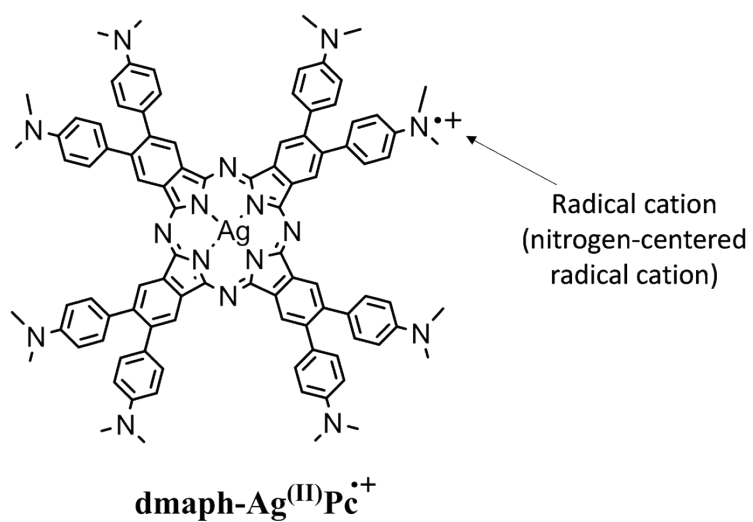


Figure S23. Structure of the radical cation $\text{dmaph-Ag}^{\text{II}}\text{Pc}^{\bullet+}$